ECMWF Feature article

METEOROLOGY

Climate variability from the new System 3 ocean reanalysis
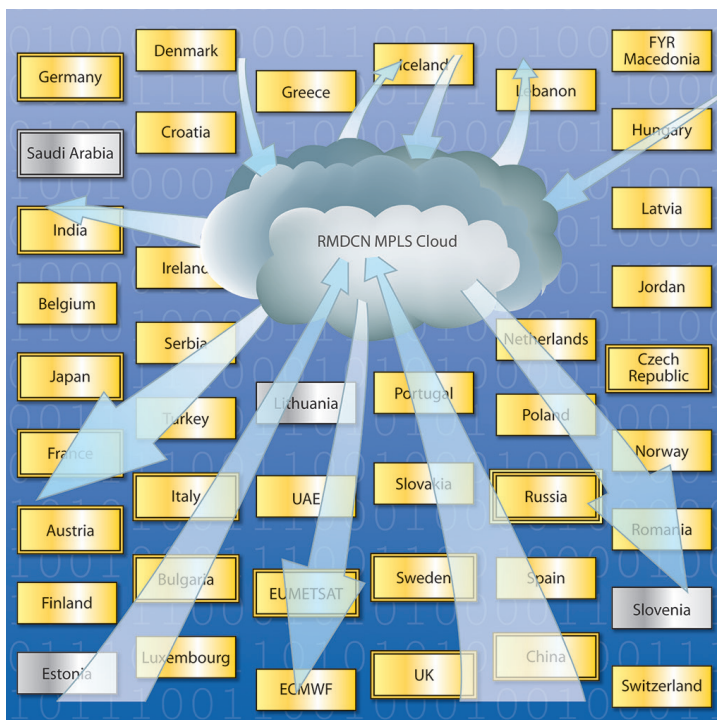
Climate variability from the new System 3 ocean reanalysis

Magdalena Alonso Balmaseda, David Anderson, Franco Molteni

In August 2006 a new ocean analysis (System 3 or S3) was implemented in operations at ECMWF. This is used to provide ocean initial conditions for the seasonal forecasts and, with some modifications, the monthly forecast system. Since both the seasonal and monthly forecast systems require an extensive set of hindcasts over many previous years, it is necessary to perform an ocean reanalysis as well. Currently a reanalysis has been performed back to 1959. Since the ocean reanalysis is an integral part of the operational system, the ocean model, resolution and assimilation procedure for the historical reanalysis are always the same as for the current operational analysis. Note that this is different from the approach used for atmospheric reanalyses such as ERA-40 in which the assimilation/model system is not necessarily the same as in the current operational system.

In addition to providing initial conditions for forecasts, the ocean reanalysis is an important resource for climate variability studies. We show that as well as improving the skill of seasonal forecasts, the S3 ocean reanalysis (hereafter denoted by ORA-S3) offers an interesting perspective on the earth's climate. The 48-year reconstruction is used to explore the amplitude, vertical penetration and geographical distribution of the ocean warming. It is also possible to estimate the steric changes in global sea level (i.e. changes in volume due to changes in the water density), which can be compared with the estimation of global sea level provided by the altimeter data since 1993.

A major concern for the historical reconstruction of the climate is the non-uniform observation coverage in time and space. To assess the robustness of the climate signals found in ORA-S3, we compare with those from an equivalent ocean experiment that is forced by atmospheric fluxes, but without assimilating ocean data. The consistency between ORA-S3 and this later experiment, called ORA-nobs hereafter, not only consolidates the significance of the ocean signals, but also provides an assessment of the quality of the atmospheric fluxes used to drive the ocean model.

The ORA-S3 system

The ORA-S3 system has several innovative features, including an on-line bias correction algorithm, the assimilation of salinity data on temperature surfaces, and assimilation of altimeter-derived sea level anomalies and global trends. A detailed description of the analysis system is provided in *Balmaseda et al.* (2007a). A selection of historical and real-time ocean analysis products can be seen at
www.ecmwf.int/ products/forecasts/d/charts/ocean/

Figure 1 shows schematically the different data streams used in the production of ORA-S3.

- *Subsurface observations.* The subsurface observations come from the quality-controlled dataset prepared for the ENACT and ENSEMBLES projects until 2004 (*Ingleby & Huddleston,* 2006), and from the Global Telecommunication System thereafter (ENACT/ GTS). Before the start of the Argo programme in 2002, the subsurface data consist mainly of profiles of temperature from XBTs (expandable bathythermographs), CTDs (conductivity-temperature-depth profiling floats) and moored arrays (TAO/TRITON and PIRATA), and a smaller number of salinity profiles from CTDs and TRITON moorings. The implementation of the Argo programme was largely completed in 2006, providing for the first time near global coverage of both temperature and salinity (*Gould,* 2005).

- *Altimeter data.* The altimeter data used are global gridded weekly maps from 1993 onwards (*Le Traon et al.,* 1998).

- *Sea surface temperatures.* The model sea surface temperatures (SSTs) are strongly relaxed to analyzed daily SST maps from the OIv2 SST product (*Reynolds et al.,* 2002) from 1982 onwards. Prior to that date, the same SST product as in the ERA-40 reanalysis was used.

The ocean data assimilation system for ORA-S3 is based on the HOPE-OI scheme. The first guess is obtained by forcing the ocean model with daily fluxes of momentum, heat and fresh water from the ERA-40 reanalysis for January 1959 to June 2002 and from the NWP operational analysis thereafter; the fresh water flux in ERA-40 has been corrected according to *Troccoli & Kållberg* (2004).
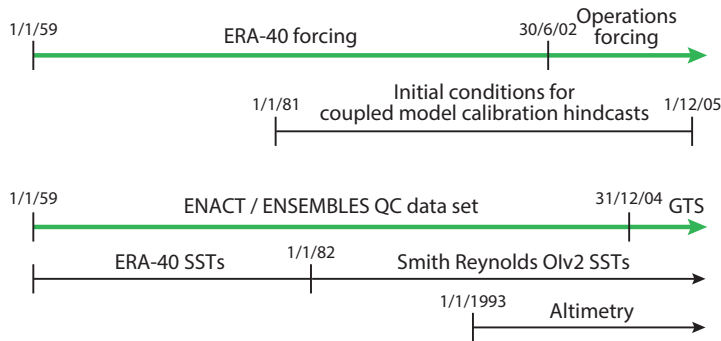
Figure 1 Data streams used in the S3 ocean reanalysis.

Since a historical reanalysis is required to initialize the calibrating hindcasts for the seasonal and monthly forecasting systems, the quality of the reanalysis will influence the calibration process, and hence the quality of the forecasts. Ideally, the ocean reanalysis should provide a reliable representation of the inter-annual variability. Often, however, the variability can be contaminated by changes in the observing system, especially if these act to correct biases in the background. In ORA-S3, the introduction of a bias-correction algorithm with both prescribed and adaptive components has improved the representation of the inter-annual variability of the upper ocean heat content (*Balmaseda et al.,* 2007b). However, there may still be problems with the representation of the variability in very poorly observed areas, such as the Southern Ocean (also known as the Antarctic Ocean or South Polar Ocean), and in the salinity field.

As for the previous operational analysis system (S2), ORA-S3 consists of an ensemble of five simultaneous reanalyses. The purpose of the multiple analyses is to sample uncertainty in the ocean initial conditions, and thereby contribute to the creation of the ensemble of forecasts for the probabilistic predictions at monthly and seasonal ranges. Five simultaneous ocean analyses are created by adding perturbations to the wind stress while the ocean model is being integrated forward in time. The perturbations are commensurate with the estimated uncertainty in the wind stress product, but the ensemble does not sample uncertainties in fresh water fluxes, heat fluxes or model formulation.

Impact of the ocean analyses on the forecast skill

The ultimate goal of the ocean reanalysis is to improve the skill of the seasonal forecasts of SST. It is important to quantify the impact of improving the ocean initialization compared with the impact of improvements in the atmosphere model.

To this end, a coupled seasonal forecast experiment has been conducted with the atmospheric model used in S3 (*Anderson et al.,* 2007), but with ocean initial conditions from the previous S2 ocean analysis. We call this experiment S2icS3m. The experiment consists of 76 ensemble forecasts, with initial conditions three months apart (January, April, July and October) spanning the period 1987–2005. For each date, an ensemble of five coupled forecasts (with perturbed initial conditions) is integrated with a lead-time of up to 7-months. The forecast SST anomalies are then computed with respect to the model climatology (which depends on the lead time).

Figure 2(a) shows the RMS error in the forecast of SST anomalies as a function of lead-time in the Niño4 area for S2icS3m, together with the results from the S3 and S2 seasonal forecasting systems which have been subsampled to cover exactly the same set of 76 forecasts as for S2icS3m. The results indicate that the impact of the improved ocean initial conditions is comparable to the impact of changing the atmospheric cycle from Cy23r4, as used in S2, to Cy31r1, as used in S3.

It is also important to quantify the improvement in the forecast skill resulting from the assimilation of ocean data. To this end, another seasonal forecast experiment has been performed using ocean initial conditions from ORA-nobs, identical to the ORA-S3 ocean analysis where no ocean data, apart from SST, has been assimilated. Everything else (spin up, SST relaxation, forcing fields etc.) is the same as in ORA-S3. As before, the experiment consists of 76 different ensemble forecasts, with initial conditions from the period 1987–2005. The coupled model is that used by S3. Results displayed in Figure 2(b) show that data assimilation significantly improves the forecasts of SST: the RMS error from forecasts using ORA-S3 is substantially smaller than that of forecasts from ORA-nobs. The improvement, more noticeable in the western Pacific, is also apparent in the Indian Ocean, eastern Pacific and subtropics. However, in regions where the forecasting system has little skill, for example the equatorial Atlantic, the assimilation of data in the ocean initialization does not lead to any noticeable improvement.
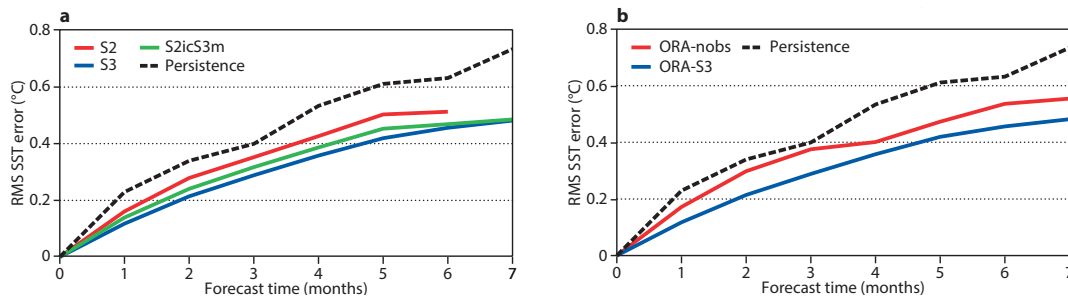
Figure 2 RMS error in the seasonal forecast of SST in the region Nino 4 (5°N–5°S, 160°E–150°W) as a function of lead-time. (a) Results from S2 (red), S3 (blue) and the hybrid S2icS3m (green). (b) Results from ORA-S3 (blue) and ORA-nobs (red) for which no ocean data has been used in the preparation of the ocean initial conditions.

Changes in the ocean heat content

Monitoring the changes in ocean heat content is important for understanding and predicting changes in the climate. *Levitus et al.,* 2005 (referred to as Levitus05 in what follows) estimate that about 84% of the increased heat stored by the Earth system during the past 50 years has been stored in the world's oceans. Their work, describing the spatial distribution of the heat storage and time evolution of the warming trends over the period 1955–2003, is an important contribution of the IPCC AR4 (*Bindoff & Willebrand,* 2007).

We now describe the evolution of the ocean heat content from ORA-S3 for the period 1959–2006 and compare the results with Levitus05 as a demonstration of the value of the ORA-S3 reanalysis for climate studies. As the variability in both Levitus05 and ORA-S3 can be affected by changes in the observing system, we also make a comparison with ORA-nobs. This comparison allows a consistency check of the climate signals in both the ocean observations and in the atmospheric forcing fluxes, as well as demonstrating the impact of assimilating ocean data.

Time evolution of the upper ocean heat content

The time evolution of the upper ocean heat content of the World Ocean (i.e. all the oceans) for the five ensemble members of ORA-S3 and estimates from ORA-nobs, as measured by the average temperature in the upper 300 m (denoted T300), are shown in Figure 3(a). As well as a clear warming trend, captured by both ORA-S3 and ORA-nobs, there is significant decadal variability, though with smaller amplitude in ORA-nobs. The coherence between ORA-S3 and ORA-nobs indicates that the variability in ORA-S3 is not simply due to changes in the oceanic observing system but must come in part from the surface forcing.

The curve for ORA-S3 in Figure 3(a) shows several features in common with Figure 1 of Levitus05. Particularly noticeable are the minimum after 1965, the local maximum around 1980 and the local minimum around 1985, more pronounced in ORA-S3 than ORA-nobs. The cooling after 1980 occurs mainly in the Pacific, in agreement with Levitus05. ORA-S3 also shows a brief stabilization of the warming around 1992, and a cooling starting in 2002. This cooling was first reported by *Lynman et al.* (2003), and has been attributed to faulty sensors in some of the Argo floats (SOLO/FSI). We refute this latter point as an additional experiment was conducted, similar to ORA-S3 but with all the SOLO/FSI data blacklisted, the results of which show that the SOLO/FSI data are not responsible for the 2002 cooling and subsequent stabilization of the warming trend. In fact there is little difference between the two experiments, probably because the bad data were rejected by the ORA-S3 quality control system in first place. Besides, in our analysis the cooling takes place in the Southern Ocean, where there were no SOLO/FSI floats. The 2002 cooling is captured in ORA-nobs, indicating that it is not an artefact of the sampling.

The stabilization of the heat content post-2003 in ORA-S3 shown in Figure 3(a) is more debatable. It does not appear in ORA-nobs, where the 2002 cooling is short-lived and warming of the upper ocean soon recommences. Additional observing system experiments, in which the Argo floats are removed, show that the post-2003 stabilization of the heat content in ORA-S3 is affected by the Argo data, since it is the first time that there is good observational coverage of the Southern Ocean.

Figure 3(b) shows the time evolution of T300 for the North Atlantic region (30°N–60°N), which is quite different from the time evolution for the World Ocean, illustrating the regional variations in the warming trends. In the North Atlantic, the warming only starts in the late 1980s, in both ORA-S3 and ORA-nobs. The warming trend is interrupted for a few years after 2000. The warming then continues in ORA-S3, reaching a peak in 2005, but there is no such warming in ORA-nobs. From various observing system experiments we have conducted, we attribute the pronounced 2005 warming in ORA-S3 to the Argo data. The evolution of sea level from altimeter data (see later) does not show any special rise during 2005 in the North Atlantic suggesting that the warming may be an artefact of nonuniform sampling.
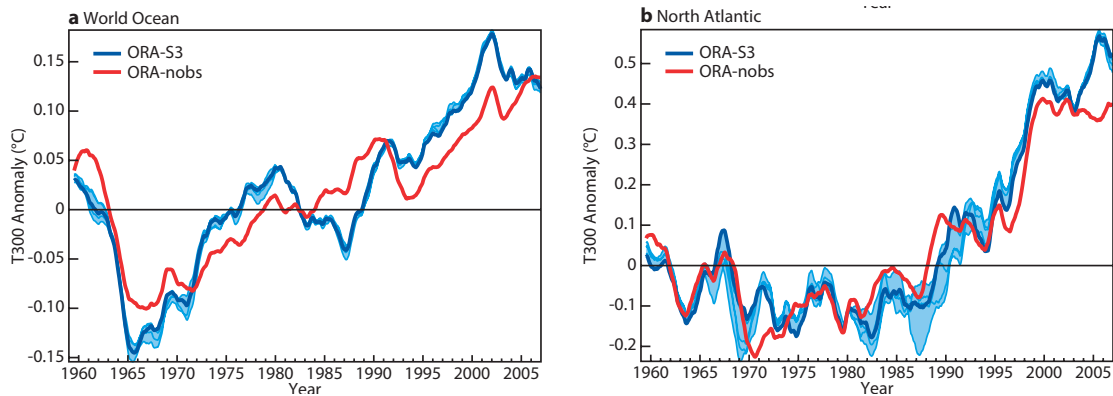
Figure 3 Time evolution of the upper ocean heat content, as measured by the averaged temperature in the upper 300 m (T300) in (a) the World Ocean and (b) in the North Atlantic (30°N–60°N). The time series show the 12-month running average anomalies, relative to the 1960–2005 climatology. The blue curves are the five ensemble members in ORA-S3 with solid blue line indicating the unperturbed analysis and the shading indicating the spread. The red curve is from ORA-nobs.

Spatial distribution of the changes

Differences between the 1983–2006 and the 1959–1982 climatologies shown in Figure 4 are used to explore the spatial distribution of the warming in SST and T300.

Figure 4(a) shows that the warming of the surface temperatures is widespread, except for a cooling in the Pacific at 40°N and a region in the Southern Ocean around 50°S. The surface warming is extensive in the Indian and Atlantic Oceans. The tropical Pacific gets warmer nearly everywhere, but not in an equatorially confined band in the eastern part of the basin. Peak values, which in places exceed 2 K, are reached in high latitudes, along the path of the Gulf Stream, the confluence of the Falkland and Brazil currents, in the Greenland-Norwegian Sea and in the southern part of the Antarctic Circumpolar Current.

The spatial patterns for T300 given in Figure 4(b) are quite different to those for SST. Below the surface, the equatorial Indian and Pacific Oceans are getting colder, especially south of the equator, a feature that does not reach the surface except for an equatorially confined band in the eastern Pacific. The warming of the SST in the tropical band is therefore quite shallow. The subsurface cooling within the 10°N–10°S latitudinal band in the Pacific and at around 10°S in the Indian Ocean is also observed in ORA-nobs, implying that it is the consequence of changes in the surface forcing, most likely in the wind stress.

Changes in the zonal and meridional wind stress are shown in Figures 4(c) and 4(d). In the Indian and Pacific basins, the equatorial easterlies are weaker in the later period, suggesting a reduction in the strength of the Walker circulation (*Vechi et al.,* 2006). The easterlies are stronger both sides of the equator, between latitudes of 5°–10°. There is a stronger convergence of the meridional component at the equator, suggestive of an intensified Hadley circulation. The weakening in the zonal winds along the equator leads to a reduced east-west slope of the equatorial thermocline and a weakening of the equatorial upwelling, mostly in the East Pacific.

The off-equatorial intensification of the trades increases the latitudinal extent of the meridional circulation cell in the ocean, with increased divergence either side of the equator and increased convergence at around 15°N/S. The net effect is an export of heat from the equator towards 15°N/S within the depth of the wind-driven meridional cell (~300 m). The cooling in the Indian Ocean south of the equator is produced by a similar mechanism. The changes in the wind stress lead to a weakening of the northern branch of the South Equatorial Current and the North Equatorial Countercurrent. That the 10°N-10°S cooling appears in ORA-nobs suggests that the signal is caused by the surface forcing. That the cooling appears in ORA-nobs and Levitis05 independently is indicative of a consistency between ocean observations and surface fluxes.

ORA-S3 also captures the cooling in the North Pacific around 40°N described in Levitus05. This cooling, apparent in both SST and T300, has been attributed to the positive phase of the Pacific Decadal Oscillation (PDO), which occurred after 1976 and led to a strengthening of the Kuroshio Extension. The cooling at 40°N is also reproduced in ORA-nobs, although with smaller amplitude. It may be related to the PDO through the intensification of the Aleutian Low. In the Southern Ocean, changes in ORA-S3 and ORA-nobs are found near the Antarctic Circumpolar Current also in agreement with the IPCC AR4. This warming has been linked to a southward shift and intensification of the westerly winds over this area. The warming is more pronounced in ORA-S3 than ORA-nobs. The largest degree of consistency between SST and T300 warming occurs in the Atlantic basin, where the warming signal occupies a large fraction of the basin. The cooling in the North Pacific is also consistent in SST and T300.
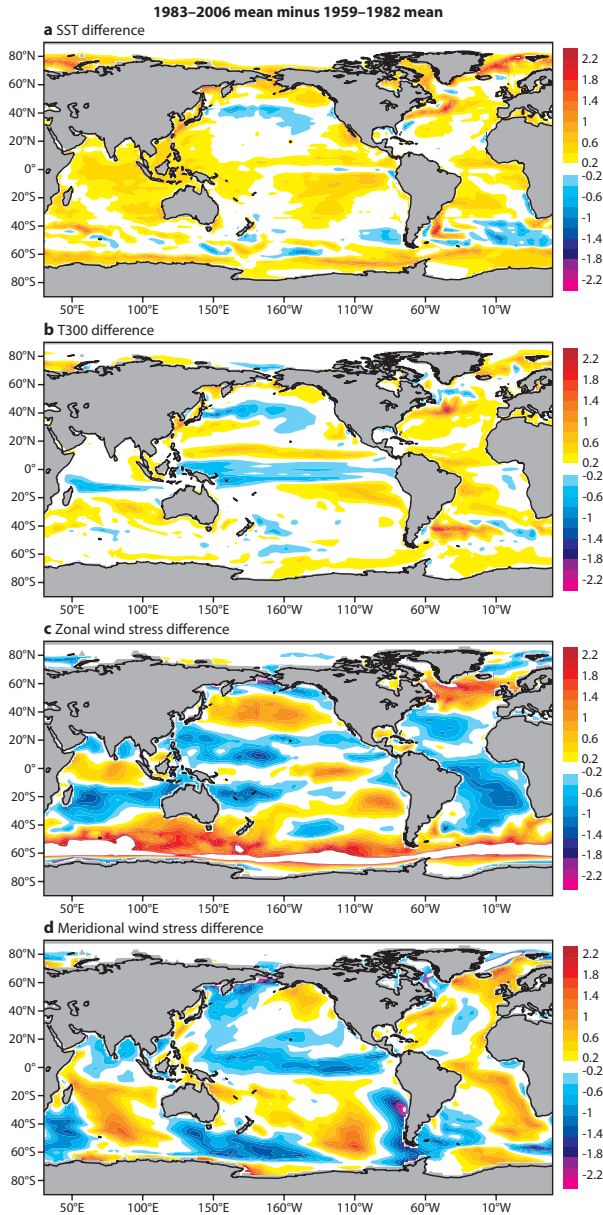
1983–2006 mean minus 1959–1982 mean

a SST difference

b T300 difference

c Zonal wind stress difference

d Meridional wind stress difference

Figure 4 Difference maps of the 1983–2006 mean minus the 1959–1982 mean for (a) SST (°C) and (b) T300 (°C). The differences in the zonal and meridional components of the wind stress $(10^{-2}\ N\ m^{-2})$ are given in (c) and (d).

Vertical structure

A better insight into the vertical distribution of the changes in temperature is given in Figure 5. This shows a depth-latitude map of the zonally averaged temperature trends over the period 1959–2006 in ORA-S3 for the Atlantic, Pacific, Indian and World Oceans. The figure is directly comparable with Figure 5.3 of the IPCC AR4 (*Bindoff & Willebrand,* 2007), using the same contour interval and shading convention. The spatial patterns in ORA-S3, although largely consistent with Levitus05, exhibit sharper vertical and meridional structures probably because the resolution used in ORA-S3 is higher, and no smoothing has been applied. Most of the changes in Figure 5 indicate warming, but interestingly there is also cooling occurring in the form of cold/warm dipoles, possibly associated with the displacement of the gyres, and also circulation changes in the equatorial Indian and Pacific Oceans.

The cooling of the equatorial cells in the Pacific and Indian Oceans is likely caused by changes in the ocean circulation. Poleward of the equatorial cooling, immediately adjacent to it and penetrating up to 400 m, there is warming, which in the Indian Ocean occurs only south of the equator. In the tropical Atlantic the cold equatorial cell is not so evident, but there is warming in the subtropics, similar to that in the Pacific. The changes in the North Pacific (40°N) may be circulation changes associated with the PDO and the strengthening of the Kuroshio Extension. The signal penetrates as deep as 600 m. Both the equatorial cells and the PDO signal in ORA-S3 are in agreement with Levitus05, although the amplitude is larger in ORA-S3. The equatorial cooling is also present in ORA-nobs, indicating that the signal is wind-driven. Curiously the signal in ORA-nobs is larger than in ORA-S3, suggesting that the wind changes are too strong or the model too sensitive.

Large changes are also apparent in the North Atlantic, with a deep and pronounced cooling around 50°N and a warming at around 40°N. Although the warming penetrates as far as 1000 m, the peak value occurs within the first 200 m. In Levitus05 the peak warming is deeper (~600 m), with a secondary maximum within the first 200 m. The cooling at 50°N is even deeper, and more intense in ORA-S3 than in Levitus05. The same dipolar structure also appears in ORA-nobs. The Atlantic is the ocean with the strongest warming and the deepest penetration.

In general, changes in the southern hemisphere are stronger in ORA-S3 than in Levitus05. Particularly noticeable is the large warming at around 40°S in the Atlantic observed in ORA-S3 but not in Levitus05. It is also much weaker in ORA-nobs. This warming is very noticeable in Figure 4(b) to the east of Argentina.
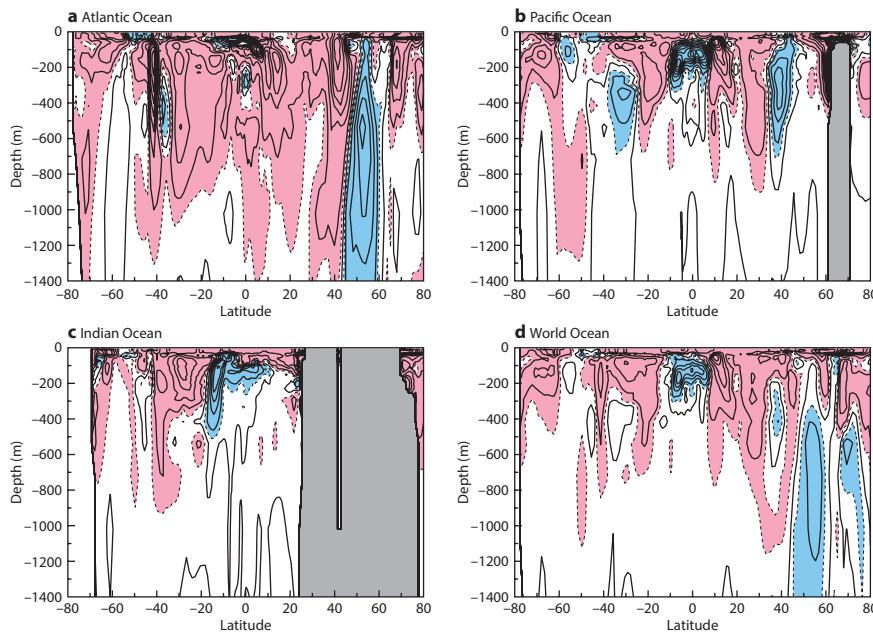

Figure 5 Latitude-depth sections of the linear trends in temperature over the period 1959–2006 in ORA-S3 for the (a) Atlantic, (b) Pacific, (c) Indian Ocean and (d) World Ocean. The contour interval is 0.05 degrees/decade. Values above 0.025 degrees/decade are shaded in pink, and those below -0.025 degrees/decade are shaded in blue. The trends are the gradients obtained from the best root mean square fit of a straight line.

Sea level change and thermal expansion

Changes in the sea level can result from two major processes that alter the volume of the water in the global ocean: steric changes (due to variations in the density of water) and the exchange of water between the ocean and other water reservoirs such as glaciers and ice sheets. Measurements of present-day sea level change rely on tide gauges and, since 1993, satellite altimetry. The steric changes can be diagnosed using analysis of temperature and salinity. The differences between global steric changes and global sea level can be used as an indication of mass variations. However, large uncertainties remain. Results summarized in the IPCC AR4 indicate that for the period 1961-2003 thermal expansion contributed only one-quarter of the estimated sea level rise, while melting of the land ice accounted for less than half. Thus, the full estimate of sea level rise cannot be accounted for. During recent years the observing system has improved, and for the period 1993-2003 it is possible to close the budget in sea level change, albeit with large uncertainties.

Here we present steric height estimations from ORA-S3 and compare them with the results in the IPCC-AR4. The geographical distribution of the linear trends in steric height for the periods 1961–2003, and 1993–2003 are shown in Figures 6(a) and 6(b). Both of them show large geographical variations but the spatial patterns differ substantially between the two periods. For the longer period, the pattern of steric height is very similar to the pattern of changes in the upper ocean heat content (Figure 4(b)). For the shorter period (Figure 6(b)), the trends in steric height in the Pacific and Indian Oceans show more zonal variability (rather than the meridional structure shown in Figure 6(a). This is in good agreement with trends in sea level from altimeter (Figure 6(c)), and resembles the negative phase of ENSO and Indian Dipole patterns. The trends are for higher sea level in the western Pacific and eastern Indian Ocean, and lower sea level in the eastern Pacific and western Indian Ocean. The trends in the Atlantic Ocean are for higher sea level almost everywhere except for the pronounced negative trend southeast of Greenland. The altimeter data also shows a region of reduced sea level in the North Atlantic although not in exactly the same location.

Figure 7 shows the evolution in global steric height from the ORA-S3 ocean analysis and for ORA-nobs. The global sea level from altimeter data is also shown starting in 1993. The time evolution of the global steric height is similar to the evolution of the global upper ocean heat content as shown in Figure 3(a): there are local minima in the mid 1960s and 1980s, followed by a rapid rise and then a sharp decrease starting in 2002. For the period 1993-2002 the sea level evolution and the steric height exhibit similar trends, except for the period around 1998 when there is a large increase in sea level not matched by the steric height. After 2002, the altimeter sea level and ORA-S3 steric height diverge considerably. In comparison, the steric height for ORA-nobs does not have the minimum in the 1980s, the increase in the period 1993–2003 is weaker and, as for T300, the post-2002 decrease in steric height is weak and short-lived. The trend for the period 1961–2003 is 0.9 mm/yr in ORA-S3, twice as large as previous estimates reported in the IPCC-AR4. It is only 0.55 mm/yr in ORA-nobs. Both ORA-S3 and ORA-nobs exhibit higher values in the steric height trends for the period 1993–2003 (2.1 and 1.1 mm/yr respectively) in agreement with the acceleration in sea level rise reported by *Church & White* (2006). The acceleration rate is stronger in ORA-S3.

The widening gap between the evolution of sea level and steric height after 2002 is worrying. The difference is even larger after 2004. The origin of this mismatch is unknown. One possibility is the underestimation of the volume increase by the ocean analysis. This could be a consequence of the changing observing system: the advent of Argo implies that for the first time there is a uniform distribution of temperature and salinity observations in the oceans of the southern hemisphere, but observing system experiments indicate that the widening gap occurs even without Argo. The mismatch could be real reflecting an increase in the mass of the oceans from the melting of glaciers and continental ice sheets. Understanding the origin of the widening gap between sea level trends and steric height trends is of paramount importance for the monitoring of the earth system and its response to global warming.
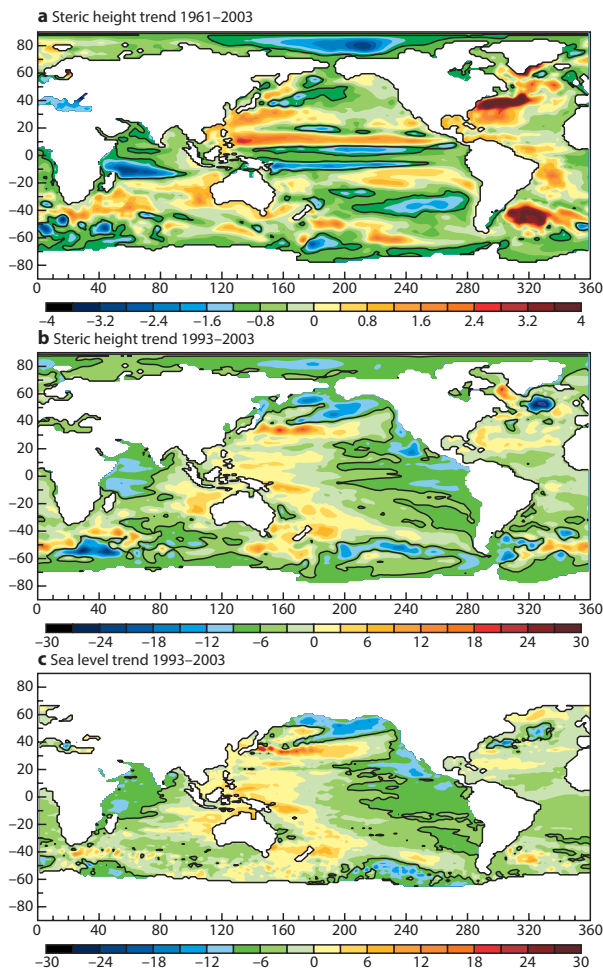

Figure 6 Spatial pattern of the linear trends in steric height changes in ORA-S3 for (a) 1959–2003 and (b) 1993–2003. (c) This shows the spatial distribution of the linear trend in sea level from altimeter data for the period 1993–2003 (c). The colour interval is 0.4 mm/yr for (a) and 3 mm/yr for (b) and (c). The zero contours are shown.
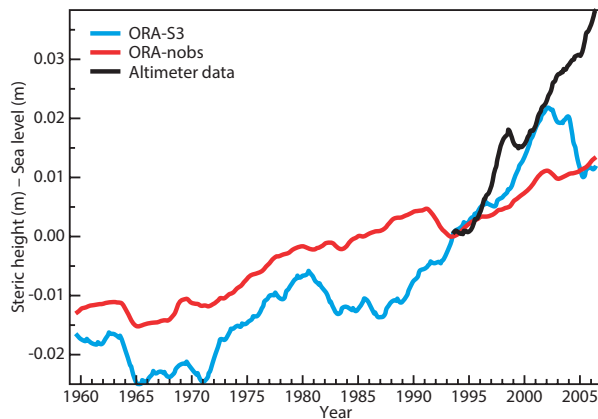
Figure 7 Time evolution of the global steric height in ORA-S3 (blue) and ORA-nobs (red) for the period 1960–2007, and the global sea level from the altimeter data (black) for the period 1993–2007. The time series are 12-month running mean, relative to the 1993 average, so the three curves have the same origin in 1993.

Summary and conclusions

We have shown that the initial conditions from the ORA-S3 ocean reanalysis produce better forecasts of SST than those from the previous operational system (S2). It is found that the effect of better ocean initialization in the forecasts of SST is of comparable magnitude to the effect of changing the atmospheric model cycle in the coupled system from that used in S2 to that used in S3. It has also been shown that assimilating ocean observations not only improves significantly the skill of the seasonal forecasts of SST, but also improves the estimation of climate signals (e.g. the distribution of warming trends in the ocean heat content and the trends in steric height).

The ORA-S3 provides a historical reconstruction of the ocean since 1959. The 48-year record has been used to investigate the distribution of the warming trends in the oceans and attribution of sea level changes due to changes in density and by inference mass. Comparisons between ORA-S3, ORA-nobs which has no assimilation of ocean data, and the Levitus05 analysis based solely on ocean observations, have been used as tests for the robustness of the climate signals. In some cases the trends in ORA-S3 have larger amplitude than either the estimates based solely on ocean observations or on ORA-nobs. This is indicative of the constructive synergy between the information provided by the ocean observations and atmospheric fluxes.

The changes in the ocean heat content are mostly shallow, occurring within the mixed layer and usually involving warming but they can penetrate deeper, up to 1000 m and involve both warming and cooling possibly associated with changes in the ocean circulation. Several important changes in the ocean circulation have taken place during the past 48 years. The equatorial meridional cell has intensified in the Pacific and Indian Oceans; apparently a consequence of changes in the winds, leading to a net cooling of the equatorial ocean in the upper 300 m and substantial changes in the equatorial current system. In the North Pacific, there is a cooling at around 40°N resulting from the intensification of the PDO. Also there is a deep meridional dipole (warming at around 40°N and cooling at 50°N) in the North Atlantic reaching depths of 1000 m. The circulation changes appear to be wind driven, and appear in ORA-nobs with smaller magnitude. The Atlantic Ocean is the basin most affected by warming trends in terms of amplitude, relative horizontal coverage and vertical penetration.

The analysis of the warming trends in the ocean has several implications for predictability studies. The time series of the upper ocean heat content shows that the warming trend is not uniform but exhibits large decadal variations with important regional variations. Understanding the origin and predictability of these decadal variations is important for future climate projections. The ocean heat content and circulation from the ocean reanalysis can also provide a metric for evaluating the quality of the climate models used for climate change predictions. Furthermore, the correct initialization of the ocean component may be important for the quality of climate predictions.

The attribution of sea level change is still an open issue: for the period 1961–2003, the rates of sea level rise given by historical reconstructions based on tide gauge and altimeter data are higher than the estimates of the steric effect from ocean temperature and salinity observations. The difference appears to be too large to be accounted for by an increase in mass due to melting of the continental ice. The steric height trends from ORA-S3 for the period 1961–2003 are 0.9 mm/yr, higher than existing reconstructions based on ocean and salinity observations, higher than in the experiment with no data assimilation, and closer to the trends in sea level from tide-gauges. ORA-S3 also captures the increase in steric height from 1993 to 2003. After 2002, the gap between sea level and steric height widens considerably for reasons that are not understood.

Further Reading

Anderson, D., T. Stockdale, M. Balmaseda, L. Ferranti, F. Vitart, F. Molteni, F. Doblas-Reyes, K. Mogensen & **A. Vidard,** 2007: Development of the ECMWF Seasonal Forecast System-3. *ECMWF Tech. Memo. No. 503.*

Balmaseda, M., A. Vidard & **D. Anderson,** 2007a: The ECMWF System-3 ocean analysis system. *ECMWF Tech. Memo. No. 508.*

Balmaseda, M., D. Dee, A. Vidard & **D.L.T. Anderson,** 2007b: A multivariate treatment of bias for sequential data assimilation: Application to the tropical oceans. *Q. J. R. Meteorol. Soc.,* **133,** 167–179.

Bindoff, N. & **J. Willebrand** (and many others) 2007: Observations: Oceanic climate change and sea level. *Chapter 5 of the IPCC 4th Assessment.* Available from http://ipcc-wg1.ucar.edu/wg1/wg1-report.html

Church, J. & **N.J. White,** 2006: A 20th century acceleration in global sea level rise *Geophys. Res. Lett.,* **33,** L01602, doi:10.1029/ 2005GL024826.

Gould, J., 2005: From Swallow floats to Argo – the development of neutrally buoyant floats. *Deep-Sea Research II,* **52/3–4,** 529–543.

Ingleby, B. & **M. Huddleston,** 2006: Quality control of ocean temperature and salinity profiles – historical and real-time data. *J. Mar. Sys.,* **65,** 158–175.

Le Traon, P.-Y., F. Nadal & **N. Ducet,** 1998: An improved mapping method of multisatellite altimeter data. *Atmos. Oceanic Technol.,* **15,** 522–534.

Levitus, S., J.I. Antonov & **T.P. Boyer,** 2005a: Warming of the World Ocean, 1955–2003. *Geophys. Res. Lett.,* **32,** L02604, doi: 10.1029/2004GL021592.

Lyman, J.M., J.K. Willis & **G.C. Johnson,** 2006: Recent cooling of the upper ocean. *Geophys. Res. Lett.,* **33,** L18604, doi: 10.1029/2006GL027033.

Troccoli, A. & **P. Kållberg,** 2004: Precipitation correction in the ERA-40 reanalysis. *ERA-40 Project Report Series, No. 13.*

Reynolds, R., N. Rayner, T. Smith, D. Stokes & **W. Wang,** 2002: An improved in situ and satellite SST analysis for climate. *J. Clim.,* **15,** 1609–1625.

Vecchi, G.A., B.J. Soden, A.T. Wittenberg, I.M. Held, A. Leetmaa & **M.J. Harrison,** 2006: Weakening of tropical Pacific atmospheric circulation due to anthropogenic forcing, *Nature,* **441,** 73–76.